

Sorption of Xenon, Methane, and Organic Solvents by a Flexible Microporous Polymer Catena-Bis(Dibenzoylmethanato)-(4,4'-bipyridyl)nickel(II)

D. V. Soldatov,[†] I. L. Moudrakovski, C. I. Ratcliffe, R. Dutrisac, and J. A. Ripmeester*

Steacie Institute for Molecular Sciences, National Research Council of Canada, Ottawa K1A 0R6, Canada

Received June 13, 2003. Revised Manuscript Received October 8, 2003

The title polymeric complex, $[\text{Ni}(\text{bipy})(\text{DBM})_2]$ (bipy = 4,4'-bipyridyl; DBM = PhCOCHCOPh^- , dibenzoylmethanate), absorbs considerable quantities of gases and organic solvents. This material presents special problems for characterization, as single crystals of suitable size could not be grown, and paramagnetism interferes with the usual NMR spectroscopic applications. To define the material adequately, an approach of structural analogy, along with the examination of the adsorbed guests by appropriate NMR techniques, was employed. The sorption of xenon follows an isotherm characteristic of microporous solids, with a plateau at 1:2 host-to-xenon molar ratio (68 mL of xenon per 1 g of sorbent) at ~60 atm. The interaction with methane (>100 atm) results in an uptake of up to 0.8 mol methane (27 mL/g). Under ambient conditions the title compound absorbs a wide range of organic solvents, up to two moles, either from the vapor or by direct contact with liquids. Structural changes range from minor adjustments to total reorganization of the polymer crystal structure. The basic structural features of the $[\text{Ni}(\text{bipy})(\text{DBM})_2] \cdot 2(\text{chlorobenzene})$ inclusion compound are anticipated to be the same as those determined by an X-ray single-crystal study of its isostructural Zn-analogue. The DBM ligands chelate the Zn centers forming equatorial planes and the bipy ligands bridge the flat $\text{Zn}(\text{DBM})_2$ units into linear polymeric chains to form a "wheel-and-axle" host motif, with guest species in the residual space. Deuterium NMR of the inclusion compound with benzene- d_6 gives direct evidence that it is an included guest in the crystalline lattice of $[\text{Ni}(\text{bipy})(\text{DBM})_2]$.

Introduction

The utilization of inclusion compounds for sensing, confining, deodorizing, storing, and stabilizing various chemical species is an attractive way of dealing with many tasks in chemistry and technology.¹ The possibility of supramolecular design of new host materials has promoted a great deal of research to produce different types of organic or metal–organic receptors and frameworks. One class of such materials has guest species entrapped (enclathrated) in molecular-size cavities; such materials are attractive for purposes where the guest must be confined.^{2–7} The release of the guest is impeded in these structures, and is accompanied by the collapse

or disintegration of the host framework. Materials of another class preserve a robust and accessible micropore structure and thus act as sorbents.^{8–21} The guest easily equilibrates between the interior pore structure and the

* Corresponding author. Fax: (613) 998-7833. E-mail: John.Ripmeester@nrc.ca.

[†] Permanent address: Institute of Inorganic Chemistry, Siberian Branch of the Russian Academy of Sciences, Novosibirsk 630090, Russia.

(1) *Comprehensive Supramolecular Chemistry*; Atwood, J. L., Davies, J. E. D., MacNicol, D. D., Vögtle, F., Eds.; Pergamon: Oxford, U.K., 1996; Vol. 3, pp 157–165, 445–449, 599; Vol. 6, pp 217–223; Vol. 7, pp 744–746; Vol. 10, pp 196–210, 417–428.

(2) Chapman, R. G.; Sherman, J. C. *Tetrahedron* **1997**, *53*, 15911–15945.

(3) Atwood, J. L.; Barbour, L. J.; Jerga, A. *Science* **2002**, *296*, 2367–2369.

(4) Yannakopoulou, K.; Ripmeester, J. A.; Mavridis, I. M. *J. Chem. Soc., Perkin Trans. 2* **2002**, 1639–1644.

(5) Martel, B.; Morcellet, M.; Ruffin, D.; Vinet, F.; Weltrowski, M. *J. Inclusion Phenom.* **2002**, *44*, 439–442.

(6) Burdukov, A. B.; Roschupkina, G. I.; Gatilov, Y. V.; Gromilov, S. A.; Reznikov, V. A. *J. Supramol. Chem.* **2002**, *2*, 359–363.

(7) Enright, G. D.; Udachin, K. A.; Moudrakovski, I. L.; Ripmeester, J. A. *J. Am. Chem. Soc.* **2003**, *125*, 9896–9897.

(8) Ung, A. T.; Gizachew, D.; Bishop, R.; Scudder, M. L.; Dance, I. G.; Craig, D. C. *J. Am. Chem. Soc.* **1995**, *117*, 8745–8756.

(9) Russel, V. A.; Evans, C. C.; Li, W.; Ward, M. D. *Science* **1997**, *276*, 575–579.

(10) Noro, S.; Kitagawa, S.; Kondo, M.; Seki, K. *Angew. Chem., Int. Ed.* **2000**, *39*, 2081–2084.

(11) Sozzani, P.; Comotti, A.; Simonutti, R.; Meersman, R.; Meersman, T.; Logan, J. W.; Pines, A. *Angew. Chem., Int. Ed.* **2000**, *39*, 2695–2698.

(12) Kristiansson, O.; Tergenius, L. E. *J. Chem. Soc., Dalton Trans.* **2001**, 1415–1420.

(13) Liao, J.-H.; Chen, P.-L.; Hsu, C.-C. *J. Phys. Chem. Sol.* **2001**, *62*, 1629–1642.

(14) Liu, Y.-H.; Lu, Y.-L.; Tsai, H.-L.; Wang, J.-C.; Lu, K.-L. *J. Solid State Chem.* **2001**, *158*, 315–319.

(15) Eddaoudi, M.; Kim, J.; Rosi, N.; Vodak, D.; Watcher, J.; O'Keeffe, M.; Yaghi, O. M. *Science* **2002**, *295*, 469–472.

(16) Noro, S.; Kitaura, R.; Kondo, M.; Kitagawa, S.; Ishii, T.; Matsuzaka, H.; Yamashita, M. *J. Am. Chem. Soc.* **2002**, *124*, 2568–2583.

(17) Seki, K. *Langmuir* **2002**, *18*, 2441–2443.

(18) Wang, Q. M.; Shen, D.; Bülow, M.; Lau, M. L.; Deng, S.; Fitch, F. R.; Lemcoff, N. O.; Semancin, J. *Microporous Mesoporous Mater.* **2002**, *55*, 217–230.

(19) Huang, L.; Wang, H.; Chen, J.; Wang, Z.; Sun, J.; Zhao, D.; Yan, Y. *Microporous Mesoporous Mater.* **2003**, *58*, 105–114.

external environment without change in the host structure as the guest can go in and out. Finally, materials of the third type exhibit flexible structures predisposed to, or preorganized for, guest inclusion.^{22–32} These materials respond to the presence of a suitable guest by expanding the lattice, thus forming cavities or channels that may be present only in vestigial form in the guest-free material.

Our recent research has focused on the design of metal–organic materials with flexible micropore structures.^{33–38} The general concept of flexible structures is well illustrated by some noncrystalline organic polymers which absorb solvents in significant quantities.^{39–52} However, these polymers do not display the propensity for easily controlled assembly–disassembly inherent to most coordination polymers.^{53–57} In our recent work⁵⁸

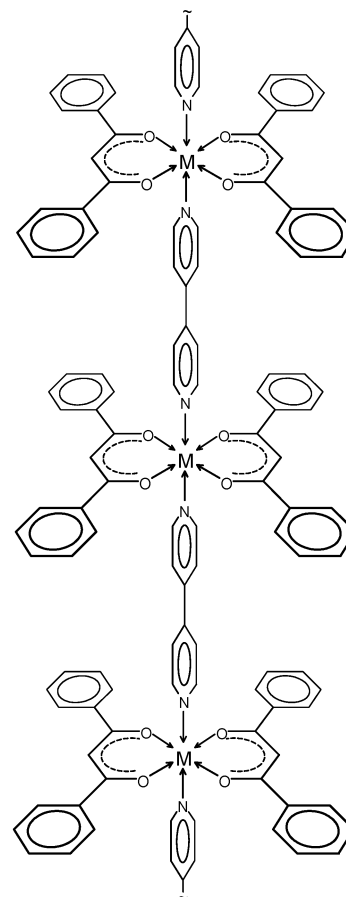


Figure 1. Structure of the $[M(\text{bipy})(\text{DBM})_2]$ polymer as found for $M = \text{Zn(II)}$ in several inclusion compounds.⁵⁸

we applied a so-called “wheel-and-axle” design^{59–64} to create 1D polymers out of flat metal(II) dibenzoyl-methanate (DBM) units bridged through 4,4′-bipyridyl (bipy) ligands. The structure of such a polymer was confirmed by single-crystal XRD analysis and is shown in Figure 1. The polymeric molecule possesses void spaces in the form of pockets located between adjacent $M(\text{DBM})_2$ units. The pockets combine into cavities or channels as dictated by the polymer chain packing in the crystal structure, and the cavity space is responsible for the ability of the bulk material to absorb guest species. This paper reports on the sorption properties

(20) Ueda, T.; Eguchi, T.; Nakamura, N.; Wasylishen, R. E. *J. Phys. Chem. B* **2003**, *107*, 180–185.

(21) Rather, B.; Zaworotko, M. J. *Chem. Commun.* **2003**, 830–831.

(22) Kitagawa, S.; Kondo, M. *Bull. Chem. Soc. Jpn.* **1998**, *71*, 1739–1753.

(23) Fletcher, A. J.; Cussen, E. J.; Prior, T. J.; Rosseinsky, M. J.; Kepert, C. J.; Thomas, K. M. *J. Am. Chem. Soc.* **2001**, *123*, 10001–10011.

(24) Halder, G. J.; Kepert, C. J.; Moubaraki, B.; Murray, K. S.; Cashion, J. D. *Science* **2002**, *298*, 1762–1765.

(25) Cussen, E. J.; Claridge, J. B.; Rosseinsky, M. J.; Kepert, C. J. *J. Am. Chem. Soc.* **2002**, *124*, 9574–9581.

(26) Lu, J. Y.; Babb, A. M. *Chem. Commun.* **2002**, 1340–1341.

(27) Uemura, K.; Kitagawa, S.; Kondo, M.; Fukui, K.; Kitaura, R.; Chang, H.-C.; Mizutani, T. *Chem. Eur. J.* **2002**, *8*, 3586–3600.

(28) Seki, K. *Phys. Chem. Chem. Phys.* **2002**, *4*, 1968–1971.

(29) Kitaura, R.; Kitagawa, S.; Kubota, Y.; Kobayashi, T. C.; Kindo, K.; Mita, Y.; Matsuo, A.; Kobayashi, M.; Chang, H.-C.; Ozawa, T. C.; Suzuki, M.; Sakata, M.; Takata, M. *Science* **2002**, *298*, 2358–2361.

(30) Suh, M. P.; Ko, J. W.; Choi, H. J. *J. Am. Chem. Soc.* **2002**, *124*, 10976–10977.

(31) Göbbitz, C. H. *Acta Crystallogr.* **2002**, *B58*, 849–854.

(32) Brouwer, E. B.; Enright, G. D.; Udachin, K. A.; Lang, S.; Ooms, K. J.; Halchuk, P. A.; Ripmeester, J. A. *Chem. Commun.* **2003**, 1416–1417.

(33) Soldatov, D. V.; Ripmeester, J. A.; Shergina, S. I.; Sokolov, I. E.; Zanina, A. S.; Gromilov, S. A.; Dyadin, Yu. A. *J. Am. Chem. Soc.* **1999**, *121*, 4179–4188.

(34) Soldatov, D. V.; Ripmeester, J. A. *Chem. Eur. J.* **2001**, *7*, 2979–2994.

(35) Nossov, A. V.; Soldatov, D. V.; Ripmeester, J. A. *J. Am. Chem. Soc.* **2001**, *123*, 3563–3568.

(36) Manakov, A. Yu.; Soldatov, D. V.; Ripmeester, J. A.; Lipkowski, J. *J. Phys. Chem. B* **2000**, *104*, 12111–12118.

(37) Soldatov, D. V.; Grachev, E. V.; Ripmeester, J. A. *Cryst. Growth Des.* **2002**, *2*, 401–408.

(38) Soldatov, D. V.; Zanina, A. S.; Enright, G. D.; Ratcliffe, C. I.; Ripmeester, J. A. *Cryst. Growth Des.* **2003**, *3*, 1005–1113.

(39) Ichiraku, Y.; Stern, S. A.; Nakagawa, T. *J. Membr. Sci.* **1987**, *34*, 5–18.

(40) Witchev-Lakshmanan, L. C.; Hopfenberg, H. B.; Chern, R. T. *J. Membr. Sci.* **1990**, *48*, 321–331.

(41) Volkov, V. V. *Polim. J.* **1991**, *23*, 457–466.

(42) Srinivasan, R.; Auvil, S. R.; Burban, P. M. *J. Membr. Sci.* **1994**, *86*, 67–86.

(43) Srisiri, W.; O'Brien, D. F.; Orådd, G.; Persson, S.; Lindblom, G. *Polym. Prepr.* **1997**, *38*, 906–907.

(44) Tsutsui, K.; Tsujita, Y.; Yoshimizu, H.; Kinoshita, T. *Polymer* **1998**, *39*, 5177–5182.

(45) Ilinitich, O. M.; Fenelonov, V. B.; Lapkin, A. A.; Okkel, L. G.; Tersikh, V. V.; Zamaraev, K. I. *Microporous Mesoporous Mater.* **1999**, *31*, 97–110.

(46) Rizzo, P.; Ruiz de Ballesteros, O.; De Rosa, C.; Auriemma, F.; La Camera, D.; Petraccone, V.; Lotz, B. *Polymer* **2000**, *41*, 3745–3749.

(47) Milano, G.; Venditto, V.; Guerra, G.; Cavallo, L.; Ciambelli, P.; Sannino, D. *Chem. Mater.* **2001**, *13*, 1506–1511.

(48) Handa, Y. P.; Zhang, Z.; Nawaby, V.; Tan, J. *Cell. Polym.* **2001**, *20*, 241–253.

(49) Hodge, K.; Prodpran, T.; Shenogina, N. B.; Nazarenko, S. J. *Polym. Sci.* **2001**, *39*, 2519–2538.

(50) Trezza, E.; Grassi, A. *Macromol. Rapid. Commun.* **2002**, *23*, 260–263.

(51) Yoshioka, A.; Tashiro, K. *Macromolecules* **2003**, *36*, 3593–3600.

(52) Loffredo, F.; Pranzo, A.; Venditto, V.; Longo, P.; Guerra, G. *Macromol. Chem. Phys.* **2003**, *204*, 859–867.

(53) *Comprehensive Supramolecular Chemistry; Templating, Self-assembly, and Self-organization*; Sauvage, J.-P., Hosseini, M. W., Eds.; Pergamon: Oxford, U.K., 1996; Vol. 9.

(54) Swiegers, G. F.; Malefetse, T. J. *Chem. Rev.* **2000**, *100*, 3483–3537.

(55) Goldberg, I. *Chem. Eur. J.* **2000**, *6*, 3863–3870.

(56) Dinolfo, P. H.; Hupp, J. T. *Chem. Mater.* **2001**, *13*, 3113–3125.

(57) Song, R.; Kim, K. M.; Sohn, Y. S. *Inorg. Chem.* **2003**, *42*, 821–826.

(58) Soldatov, D. V.; Tinnemans, P.; Enright, G. D.; Ratcliffe, C. I.; Diamante, P. R.; Ripmeester, J. A. *Chem. Mater.* **2003**, *15* (20), 3826–3840.

(59) Toda, F.; Akagi, K. *Tetrahedron Lett.* **1968**, *9*, 3695–3698.

(60) Hart, H.; Lin, L.-T. W.; Ward, D. L. *J. Am. Chem. Soc.* **1984**, *106*, 4043–4045.

(61) Jetti, R. K. R.; Kuduva, S. S.; Reddy, D. S.; Xue, F.; Mak, T. C. W.; Nangia, A.; Desiraju, G. R. *Tetrahedron Lett.* **1998**, 913–916.

(62) Caira, M. R.; Nassimbeni, L. R.; Toda, F.; Vujovic, D. *J. Chem. Soc., Perkin Trans. 2* **1999**, 2681–2684.

(63) Jetti, R. K. R.; Xue, F.; Mac, T. C. W.; Nangia, A. *J. Chem. Soc., Perkin Trans. 2* **2000**, *39*, 1223–1232.

(64) Diskin-Posner, Y.; Patra, G. K.; Goldberg, I. *J. Chem. Soc., Dalton Trans.* **2001**, 2775–2782.

of polymeric [Ni(bipy)(DBM)₂] as characterized by a range of experimental methods.

Experimental Section

Synthesis of [Ni(bipy)(DBM)₂]. *Polymorph I.* Light-green Ni(DBM)₂ (3.03 g, 6 mmol), prepared as described elsewhere,⁶⁵ was dissolved in warm tetrahydrofuran (200 mL). Bipy (0.94 g, 6 mmol) dissolved in warm tetrahydrofuran (80 mL) was added to the filtered solution with vigorous stirring. The mixture was stirred for 30 min with heating, and left to cool for 24 h. A light-green precipitate of the complex started to form 1 or 2 min after the addition and subsequently transformed into yellowish-green inclusion compound with tetrahydrofuran. The product was isolated and allowed to lose guest tetrahydrofuran in air for 1 h to give light-green [Ni(bipy)(DBM)₂] (3.64 g, 5.5 mmol; yield 90%). Elemental analysis (%). Calcd for [Ni(bipy)(DBM)₂] (C₄₀H₃₀N₂NiO₄): C, 72.64; H, 4.57; N, 4.24. Found: C, 72.53; H, 4.44; N, 4.24.

Polymorph II. A sample of [Ni(bipy)(DBM)₂] (200 mg) prepared as described above was used in the isopiestic method (see below) to prepare a 1:2 inclusion compound with acetone. Decomposition of this inclusion compound in air yielded another polymorph of the [Ni(bipy)(DBM)₂] complex, as judged from powder XRD. Elemental analysis (%). Found: C, 72.52; H, 4.51; N, 4.19.

Inclusion Compounds of [Ni(bipy)(DBM)₂] with Organic Solvents. *Isopiestic Method.* Samples of [Ni(bipy)(DBM)₂] (150 mg, polymorph I) were placed in closed vessels in an atmosphere of the desired guest solvents at room temperature. Three observations indicated the reaction of the solid host with guest vapors: (1) a color change, either yellowing or greening of the initial light-green host material; (2) a change of the powder XRD pattern; (3) a weight increase. The reactions lasted from several hours to several days. More details of the method are given elsewhere.^{33,34,66,67}

Direct Contact Method. Samples of [Ni(bipy)(DBM)₂] (300 mg, polymorph I) were equilibrated with liquid guest solvents (10 mL) for several hours. Changes in color and powder XRD pattern were usually observed. The products were separated from the solvents, dried with blotting paper until solvent marks did not show on the paper, and analyzed as such.

Measurement of Guest Content. The inclusion compounds were analyzed using three methods. *Method A:* The weight increase observed in the isopiestic method was used to calculate the number of moles of absorbed guest, although the values were less precise than usually obtained by this method.⁶⁶ This lower reproducibility may well be attributable to the easy escape of guest from the micropores. *Method B:* Samples obtained by the direct contact method were analyzed by TGA. The thermograms showed that all of the guest was lost below 130 °C, and a plateau corresponding to the host complex that was stable to over 300 °C. *Method C:* Large-scale samples (>2 g) obtained by the direct contact method were allowed to decompose in air, and the guest content was estimated from the weight loss.

Crystalline [Zn(bipy)(DBM)₂]*2(Chlorobenzene). This inclusion compound was obtained as a white crystalline material by crystallization of Zn(DBM)₂ (256 mg, 0.5 mmol, synthesis as described elsewhere⁶⁵) and bipy (86 mg, 0.55 mmol) from neat chlorobenzene (15 mL). By TGA the product showed a mass loss of 25.2% (in the 64–86 °C range; 25.2% was expected for 2 mol of chlorobenzene from the 1:2 inclusion compound). By comparing PXRD patterns of this product and that obtained by direct contact of [Ni(bipy)(DBM)₂] with chlorobenzene, the two inclusion compounds were seen to be isostructural. A single crystal of [Zn(bipy)(DBM)₂]*2-(chlorobenzene) for XRD study was picked from under the

Table 1. Crystal Data and Structure Refinement for [Zn(bipy)(DBM)₂]*2(Chlorobenzene)

gross formula	C ₄₀ H ₃₀ N ₂ O ₄ Zn, 2(C ₆ H ₅ Cl)
refined guest-to-host ratio	1.98(1)
formula weight	893.1
temperature, K	173
crystal system	monoclinic
space group	<i>P</i> 2 ₁ / <i>n</i>
unit cell parameters:	
<i>a</i> , Å	10.711(2)
<i>b</i> , Å	19.313(3)
<i>c</i> , Å	21.580(3)
β , deg	97.01(1)
<i>V</i> , Å ³	4431(1)
<i>Z</i>	4
calculated density, g cm ⁻³	1.339
absorption coefficient (Mo K α), cm ⁻¹	7.23
number of unique reflections:	
used (<i>I</i> > 0)	11408
intense (<i>I</i> > 2 σ (<i>I</i>))	9135
number of refined parameters	679
<i>R</i> values	
<i>R</i> _{int} (all data)	0.026
<i>R</i> 1 = $\sum F_o - F_c / \sum F_o $	0.033
(intense data)	
<i>wR</i> 2 (intense data)	0.083
goodness-of-fit on <i>F</i> ²	1.027
residual extrema max/min, e Å ⁻³	+0.44/−0.59

mother liquor and was cooled to −100 °C, at which temperature all further measurements were conducted.

General Methods. *TGA Measurements.* A 2050 thermogravimetric analyzer (TA Instruments) was utilized. Sample sizes were 15–25 mg, heating rate was 5° per min., and purge gas was nitrogen.

Microscope. A Weiss optical microscope equipped with a Hitachi CCTV camera was used to observe the shape and size of microcrystals picked from reaction mixtures. Magnifications were 100× or 400×.

PXRD. Measurements were done on a Rigaku Geigerflex diffractometer with Co K α radiation (λ = 1.7902 Å) in the 5–30° 2 θ range, with a 0.02° step scan with 1 or 2 s per step. Inclusion compounds were studied at room temperature in an atmosphere of the corresponding guest, to prevent dissociation. Cold samples of the inclusion compound with methane were placed on a thermostated copper holder at liquid nitrogen temperature and were studied over a range of increasing temperatures.

Single-Crystal XRD. A Bruker SMART CCD X-ray diffractometer (Mo K α radiation, λ = 0.71073 Å, graphite monochromator) equipped with an LT-2A low-temperature device was utilized. The data set for [Zn(bipy)(DBM)₂]*2-(chlorobenzene) was collected at 173 K using the ω scan mode over the 2 θ range of 2–60°. Coverage of the unique sets was over 99%. The integration of the diffraction profiles and an empirical absorption correction utilized the SAINT and SADABS routines, respectively, associated with the Bruker diffractometer. The unit cell parameters were refined using entire data sets.

The structure was solved and refined using the SHELXTL package,⁶⁸ by direct methods, followed by differential Fourier syntheses. The structural refinement was performed on *F*² using all data with positive intensities. The site occupancy of the guest molecules was refined but was fixed at 100% in the final cycles of refinement as the deviations were insignificant. Selected crystal data and experimental parameters are summarized in Table 1. Further experimental details, as well as full lists of derived results, are given in the Supporting Information (CIF).

Xe Sorption Experiments. To detect Xe absorbed in microporous [Ni(bipy)(DBM)₂], ¹²⁹Xe NMR spectroscopy was utilized. All ¹²⁹Xe NMR spectra were taken on a Bruker DSX-

(65) Soldatov, D. V.; Henegouwen, A. T.; Enright, G. D.; Ratcliffe, C. I.; Ripmeester, J. A. *Inorg. Chem.* **2001**, *40*, 1626–1636.

(66) Soldatov, D. V.; Ripmeester, J. A. *Chem. Mater.* **2000**, *12*, 1827–1839.

(67) Ipsen, H. *Ber. Bunsen-Ges. Phys. Chem.* **1998**, *102*, 1217–1224.

(68) Sheldrick, G. M. *SHELXTL PC, Ver. 4.1. An Integrated System for Solving, Refining and Displaying Crystal Structure from Diffraction Data*; Siemens Analytical X-ray Instruments, Inc.: Madison, WI, 1990.

400 spectrometer (magnetic field 9.4 T, resonance frequency at 110.6 MHz). Two types of experiments were performed: (i) with samples in a continuous flow of hyperpolarized (HP) ^{129}Xe ,^{69,70} where the greatly enhanced sensitivity of HP Xe makes it possible to observe the NMR of Xe at very low concentrations; and (ii) with samples sealed in glass tubes with Xe gas (NMR using thermally polarized ^{129}Xe). Experiments (i) and (ii) are described below.

(i) The continuous flow (CF) system for production of hyperpolarized (HP) xenon has been described elsewhere.⁷¹ A xenon–helium–nitrogen mixture with a volume composition of 1%–98%–1% was used in all CF HP experiments. The flow rate was monitored with a Vacuum General flow controller (model 80-4) and kept constant in the range of 40–60 scc/min (scc/min–gas flow normalized to standard conditions). In CF HP experiments a flow of HP xenon was delivered directly into the coil region of a modified solid-state probe (Morris Instrument Inc). The reported ^{129}Xe NMR chemical shifts were referenced to xenon gas extrapolated to zero pressure.

(ii) To prepare a sealed sample, approximately 20–50 mg of [Ni(bipy)(DBM)₂] (polymorph I) was placed into a 5-mm o.d. glass tube about 40 mm long, which had been evacuated at 100 °C for 1 h, and then loaded with a known amount of xenon gas (Matheson, ^{129}Xe natural isotopic abundance 26.4%). The packed material occupied about one-half of the tube. This geometry made it possible to perform quantitative measurements of both the amount of xenon adsorbed in the material and the density of xenon in the gas phase. First, a spectrum was obtained with the sample tube positioned such that all of the material was inside the NMR coil. Then the tube was shifted, and only the signal from the gas phase was recorded. The amount of adsorbed xenon was found by comparing the observed signal with the signal of a known quantity of xenon adsorbed in NaY zeolite. The density of the gas phase was found from its chemical shift.⁷² All spectra for the sealed samples were recorded using a Morris Instrument Inc. solid-state 5-mm NMR probe. A spin–echo pulse sequence was employed to avoid distorting the line shapes.

Methane Sorption Experiments. Samples of [Ni(bipy)(DBM)₂] (200–400 mg, polymorph I) were degassed under vacuum at 373 K for 2 h and placed in a steel bomb. The bomb was filled with methane under high pressure (~120 atm) and closed. The contents were equilibrated at 298, 333, 373, or 423 K for 20–40 h; at 333 K the pressure inside the bomb reached a constant value after ~15 h. The bomb then was cooled in liquid nitrogen and the samples were recovered and studied.

To determine the quantity of adsorbed methane, the frozen samples were placed in a thermostatically controlled vessel connected to a manometer and an expansion reservoir. All the volumes were calibrated. The samples were evacuated (<0.1 Torr) for several minutes at liquid nitrogen temperature to remove free methane (methane vapor pressure is 10 Torr at 77 K). The samples were then allowed to warm and release the adsorbed methane. The total pressure in the system was monitored as a function of temperature. After dissociation was complete, water vapor that condensed on the sample during sample transfer was frozen out and the total quantity of methane released from the sample was calculated from the residual vapor pressure in the system and the volume of the system. The residue of guest-free [Ni(bipy)(DBM)₂] complex was weighed and the composition of the initial sample was calculated.

Deuterium NMR. The samples of [Ni(bipy)(DBM)₂]**x*(C₆D₆) were prepared by the direct contact method. One sample (A) was dried superficially on filter paper and sealed immediately in an NMR tube, while the second sample (B) was sealed after allowing some of the benzene to escape.

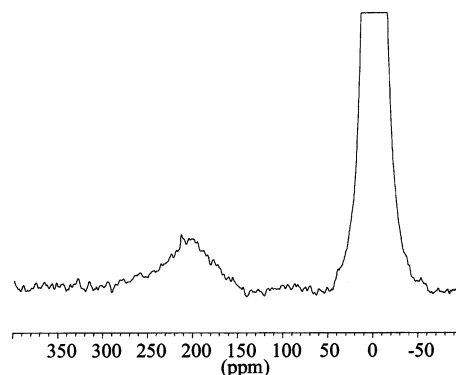


Figure 2. ^{129}Xe NMR spectrum of a sample of [Ni(bipy)-(DBM)₂] (polymorph I) in a continuous flow of gas containing hyperpolarized xenon (298 K).

Solid-state ^2H NMR spectra were obtained on a Bruker AMX-300 NMR spectrometer at 46.05 MHz using a quadrupole echo technique,⁷³ with 90° pulse lengths of 2.7 μs and recycle times of 0.35 s. Temperatures down to 125 K were achieved with a cold nitrogen flow system and a Eurotherm temperature controller. Spectra at 77 K were obtained by submerging the coil and sample in a bath of liquid nitrogen.

Results and Discussion

Sorption of Xe. Experiments with hyperpolarized Xe indicated that both polymorphs I and II of [Ni(bipy)-(DBM)₂] absorb Xe, as evident from the appearance of a strong signal in the ^{129}Xe NMR spectra at ~205 ppm. The absorption of significant quantities of Xe at a low partial pressure of Xe (~8 Torr) in the flowing gas mixture is evidence that micropore space is available in the materials and that exchange between the micropores and the gas phase is relatively easy.

Figure 2 shows the CF HP ^{129}Xe NMR spectrum of xenon in [Ni(bipy)(DBM)₂] (polymorph I) obtained at 298 K. Despite the fact that the material is paramagnetic and the expected spin–lattice relaxation time for xenon is very short, a reasonably strong signal can be detected in a very short time. At such low partial pressure (~8 Torr) the contribution of Xe–Xe interactions to the chemical shift is negligible, and the main contribution to the observed shift of xenon is from interactions with the porous material. The signal is centered slightly higher than 200 ppm and, although it cannot be said conclusively because of the weak signal-to-noise ratio, it appears to have a chemical shift anisotropy. The shift is similar to values observed for xenon adsorbed in the pores of diamagnetic molecular sieves such as zeolites, e.g., for xenon trapped in the side pockets of mordenite,^{74,75} or in xenon trapping sites in cyclodextrins, clathrasils, and clathrate hydrates (for Xe chemical shifts in molecular sieves, etc., see reviews in refs 76–79). However, it is not possible to use the shift as an

(73) Davis, J. H.; Jeffrey, K. R.; Bloom, M.; Valic, M. I.; Higgs, T. P. *Chem. Phys. Lett.* **1976**, *42*, 390–394.

(74) Ripmeester, J. A. *J. Magn. Res.* **1984**, *56*, 247–253.

(75) Nagano, J.; Eguchi, T.; Asanuma, T.; Masui, H.; Nakayama, H.; Nakamura, N.; Derouane, E. G. *Microporous Mesoporous Mater.* **1999**, *33*, 249–256.

(76) Raftery, D.; Chmelka, B. F. *NMR* **1994**, *30*, 111–158.

(77) Ratcliffe, C. I. *Annu. Rep. NMR Spectrosc.* **1998**, *36*, 124–221.

(78) Springuel-Huet, M. A.; Bonardet, J. L.; Gedeon, A.; Fraissard, J. *Magn. Reson. Chem.* **1999**, *37*, S1–S13.

(79) Barrie, P. J.; Klinowski, J. *Prog. NMR Spectrosc.* **1992**, *24*, 91–108.

(69) Grover, B. C. *Phys. Rev. Lett.* **1978**, *40*, 391–392.

(70) Happer, W.; Miron, E.; Schaeffer, S.; Schreiber, D.; Van Wijngaarden, W. A.; Zeng, X. *Phys. Rev. A* **1984**, *29*, 3092–3110.

(71) Moudrakovski, I. L.; Lang, S.; Ratcliffe, C. I.; Simard, B.; Santyr, G.; Ripmeester, J. A. *J. Magn. Res.* **2000**, *144*, 372–377.

(72) Jameson, C. J.; Jameson, A. K.; Cohen, S. M. *J. Chem. Phys.* **1973**, *59*, 4540–4546.

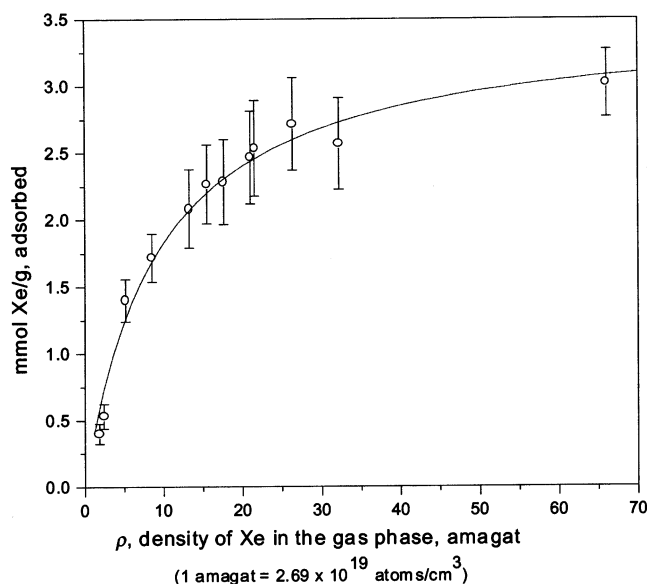


Figure 3. Sorption isotherm (298 K) of Xe in [Ni(bipy)(DBM)₂] (polymorph I). Circles with bars indicate experimental data with standard deviations from the mean of four measurements. The solid line shows a fit using a standard equation for the Langmuir isotherm (see text).

indicator of the trapping site size, as the contribution of paramagnetic Ni(II) to the chemical shift is not known.

Experiments conducted with sealed samples of polymorph I indicate that the quantity of absorbed Xe depends on pressure, as shown in Figure 3. The data show continuity over the full range of applied Xe pressures. The data are well approximated with an isotherm of Type I in Brunauer's classification,⁸⁰ characteristic of solids containing micropores.⁸¹ This shows that the host material keeps its porosity permanently even in the absence of included species. Increasing sorption in the micropores causes a sharp rise of the isotherm, which then levels off to a plateau corresponding to a saturation value. The isotherm is well described by a Langmuir equation written as $x = x_{\max}[K\rho/(1 + K\rho)]$, where x is an equilibrium (absorbed Xe):(host sorbent) mole ratio at a density ρ of Xe in the gas phase, x_{\max} is the maximum value of x , and K is a sorption constant. Derived from this, x_{\max} equals 2.3(3) (3.5(5) mmol of Xe per gram of sorbent) and $K = 0.11(1)$ (amagat)⁻¹. Assuming that each Xe atom occupies an area $\sigma = 18 \text{ \AA}^2 = 18 \times 10^{-20} \text{ m}^2$ on a surface, the specific surface area⁸¹ is $(x_{\max}N_A/M)\sigma = 377 \text{ m}^2/\text{g}$ ($N_A = 6.023 \times 10^{23}$ molecules/mol is the Avogadro constant, $M = 661.4 \text{ g/mol}$ is the molar mass of [Ni(bipy)(DBM)₂]). The material therefore is equivalent to an adsorbent with surface area of 377 m²/g with respect to Xe.

Changes in the ¹²⁹Xe NMR spectra with loading for the sealed samples are shown in Figure 4. It is apparent that the signals observed for the samples with lower loadings are not isotropic. At the smallest concentration of Xe the spectrum can be fitted with an isotropic shift of $\delta_i = 216 \text{ ppm}$, anisotropy $\Delta\delta = 70 \text{ ppm}$, and asym-

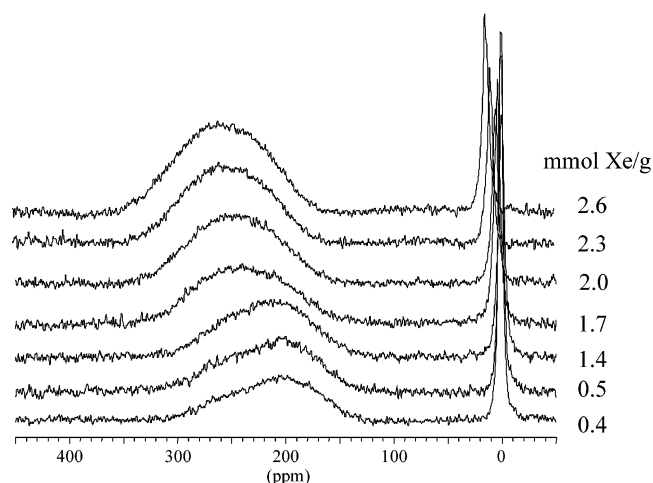


Figure 4. ¹²⁹Xe NMR spectra of sealed samples of [Ni(bipy)(DBM)₂] (polymorph I) at various xenon loadings (mmol of Xe per g of the sorbent).

metry parameter $\eta = 0.6$. One needs to note that due to extensive broadening (this assumes that the collective interaction with paramagnetic Ni(II) can be treated as a general broadening of the Xe powder pattern), fitting of the signal is not very accurate. The line shape degrades further and fitting would not be very meaningful for the higher loadings. For this reason we have not attempted a quantitative description of the line shape. Qualitatively, above 0.4 mmol Xe/g there is a gradual increase of intensity centered at about 250 ppm, which becomes dominant in the 1.7 mmol Xe/g (1.1 Xe to host polymeric unit molar ratio) spectrum. Above 2 mmol Xe/g the signal changes very little. It thus appears that there are two overlapped line shapes, and that one grows at the expense of the other as loading increases. A clue as to the actual situation may come from comparing the current results with those for Dianin's compound where two xenon atoms can "see" each other in the double-sided cavity.⁸² There, the static Xe spectrum consists of two overlapping powder patterns, and these can be attributed to singly and doubly occupied cages. Naturally, the pattern for the single xenon atom will predominate at low loading, but is easily overwhelmed by the second pattern as the loading increases, especially as doubly occupied cages give twice the signal intensity of singly occupied cages, and eventually disappears as the majority of cages become doubly occupied. Such a model may well explain the observation for the [Ni(bipy)(DBM)₂] compound. It has been shown that easily exchanging Xe atom clusters in a channel give much more complicated powder patterns that change continuously with increasing loading.^{83,84} Even sites that may accommodate three or more xenon atoms without intersite exchange show complex loading patterns, for example, NaA zeolite.⁸⁵ The best model for [Ni(bipy)(DBM)₂] then has the Xe atoms located in cavities that can be doubly occupied and that are

(82) Lee, F.; Gabe, E.; Tse, J. S.; Ripmeester, J. A. *J. Am. Chem. Soc.* **1988**, *110*, 6014–6019.

(83) Ripmeester, J. A.; Ratcliffe, C. I. *J. Phys. Chem.* **1995**, *99*, 619–622.

(84) Moudrakovski, I. L.; Ratcliffe, C. I.; Ripmeester, J. A. *Appl. Magn. Reson.* **1996**, *10*, 559–574.

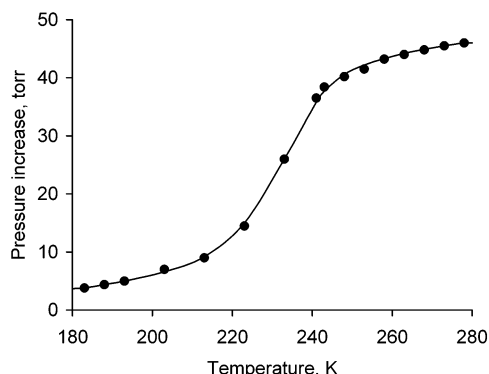
(85) Jameson, A. K.; Jameson, C. J.; Gerald R. E., II. *J. Chem. Phys.* **1994**, *101*, 1775–1786.

(80) Brunauer, S. *The Adsorption of Gases and Vapors*; Princeton University Press: Princeton, NJ, 1943; Vol. I.

(81) Webb, P. A.; Orr, C. *Analytical Methods in Fine Particle Technology*; Micromeritics Instrument Corporation: Norcross, GA, 1997; Chapter 3.

Table 2. Experimental Conditions and Results of the Methane Sorption Experiments with Sorbent [Ni(bipy)(DBM)₂] (Polymorph I)

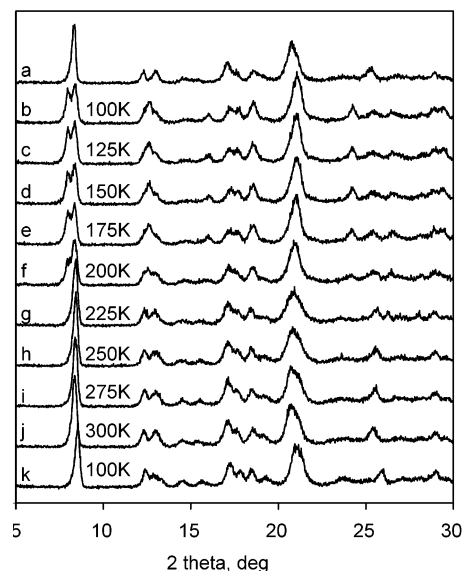
experiment	host sample mass (mg)	sorption reaction conditions	decomposition temperature interval (K)	released methane: moles per mole of host complex
1	186	20 h at 298 K, 120 atm	205–240	0.66(6)
2	276	40 h at 333 K, 123 atm	210–240	0.40(6)
3	238	30 h at 333 K, 110 atm	210–240	0.71(7)
4	259	30 h at 373 K, 127 atm	200–240	0.75(8)
5	169	40 h at 423 K, 120 atm	205–245	0.35(4)

**Figure 5.** Methane release upon warming from a sample (no. 2 in Table 2) of the [Ni(bipy)(DBM)₂] complex (276 mg of polymorph I subjected to a methane pressure of 110 atm. for 40 h at 333 K, then frozen down to 77 K). The plot shows the pressure increase in a control reservoir vs temperature as the sample is warmed at a heating rate of 4 K/min. The stepwise methane release between 200 and 240 K corresponds to 0.4 mol of methane per [Ni(bipy)(DBM)₂] unit.

relatively isolated from each other. This is also consistent with the observation that fluorobenzene can fit in the [Ni(bipy)(DBM)₂] cavity without distorting the lattice as judged from PXRD measurements (see below): for Dianin's compound, the double cavity can hold a single-substituted benzene molecule,⁸⁶ or two xenon atoms or other small guest species.

Sorption of Methane. All of the experiments carried out indicated that the title material sorbed methane at elevated pressures, as shown by data for selected experiments shown in Table 2. The quantity of absorbed methane is in the range of 0.4–0.8 mol per mol of [Ni(bipy)(DBM)₂] (9–18 mL per one g of the host complex). The experimental errors are rather large, and difficulties associated with the high-pressure experiments make it impossible at this time to find out which factor defines the quantity of absorbed gas. Nevertheless, the experiments indicate that the gas uptake is significant and takes place over a range of experimental conditions.

Figure 5 illustrates methane gas release from a quenched sample upon warming. The gas release starting at about 205 K was reproducible for all of the samples. Figure 6 shows a series of powder diffractograms of a quenched sample as it was warmed from 100 K to room temperature. This experiment confirms that the inclusion compound with methane dissociates above 200 K. It can be seen clearly that there is a structural change between the guest-free form of the sorbent (Figure 6, pattern a) and the inclusion compound with methane (Figure 6, patterns b–f). The changes in the diffraction patterns, although defined well enough, are

**Figure 6.** Powder diffractograms of (a) [Ni(bipy)(DBM)₂], polymorph I (RT); (b–j) a sample of the complex subjected to methane pressure (sample no. 2 in Table 2; 110 atm, 30 h at 333 K, then frozen down to 77 K) upon stepwise warming from 100 to 300 K; (k) the same sample frozen back to 100 K. Note the slight phase changes occurring between 200 and 225 K, which are due to methane release as the pattern does not revert upon repeated cooling to 100 K.

not severe and consist of a splitting of the reflection at $\sim 8.5^\circ$, increasing intensity of the reflection at $\sim 12.5^\circ$, and the appearance of a new reflection at $\sim 24.2^\circ$. It seems as though the structure keeps its basic architecture but undergoes some changes to accommodate methane molecules. These changes may include slight rearrangements of parallel polymeric chains and conformational adjustments of the polymeric molecules themselves. Above 200 K the structure returns to the original guest-free host phase (Figure 6, cf. pattern a and patterns g–j).

Inclusion Compounds with Organic Solvents.

The [Ni(bipy)(DBM)₂] polymer readily interacted with a wide range of organic solvents via both the vapor and liquid phases; some results are listed in Table 3. The quantities of absorbed solvents were significant, in most cases roughly two moles of guest for one host monomer unit. The accuracy of the compositions determined was lower than is usually obtained with the methods utilized, as all of the products were powdery substances that formed and decomposed easily. Solvents consisting of similarly shaped molecules transformed the polymer into the same inclusion structures (e.g., toluene and chlorobenzene) but the entire range of solvents studied produced, as judged from PXRD patterns, a variety of different inclusion structures. Some solvents (e.g., fluorobenzene) were absorbed with only slight change in the PXRD pattern, suggesting that the guest is included

(86) Enright, G. D.; Ratcliffe, C. I.; Ripmeester, J. A. *Mol. Phys.* **1999**, *97*, 1193–1196.

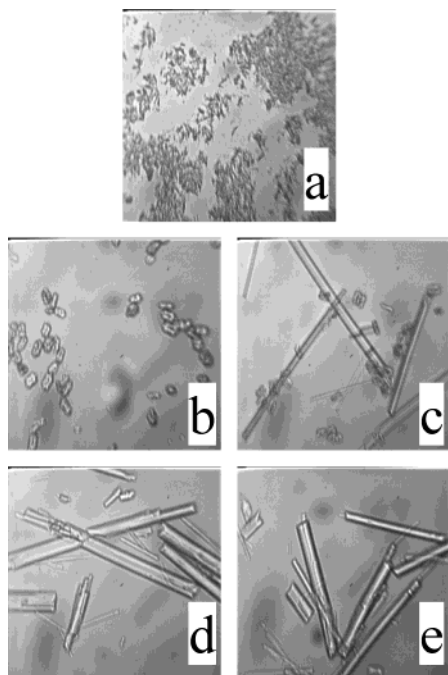


Figure 7. Transformations of $[\text{Ni}(\text{bipy})(\text{DBM})_2]$ (polymorph I) in bromobenzene at 50 °C at different times: (a) initial sample; (b) 5 min, (c) 10 min, (d) 15 min, and (e) 3 days of interaction. The size of each frame is $180 \times 180 \mu\text{m}$.

Table 3. Sorption of Organic Solvents with $[\text{Ni}(\text{bipy})(\text{DBM})_2]$ (Polymorph I): Composition, Structural Type, and Color Change of Products

guest	guest-to-host ratio (method) ^a	structural type from powder XRD	color change
benzene	>2.0 ^b	III	yellowing
toluene	2.3 (A); 2.1 (B)	IV	yellowing
chlorobenzene	2.0 (B)	IV	yellowing
<i>o</i> -xylene	1.9 (B)	V	insignificant
<i>m</i> -xylene	1.9 (B)	V	insignificant
<i>p</i> -xylene	2.0 (B)	V → IV	yellowing
methylene chloride	2.1 (A)	VI	greening
chloroform	2.1 (A)	VI	greening
tetrahydrofuran	2.4 (C)	VII	yellowing
acetone	2.0 (A)	VIII	yellowing
ethanol	1.3 (A)	IX	yellowing
fluorobenzene	0.7 (A)	I ^c	insignificant
ethyl acetate	0.4 (A)	I ^c	insignificant

^a Description of the methods is given in the Experimental Section. Experimental errors: 0.1–0.15 (method A), 0.1 (method B), 0.1 (method C). ^b Rough estimate—see discussion of the deuterium NMR results. ^c Powder pattern is similar but not identical to that of initial host form (polymorph I).

without structural reorganization of the host phase. Color changes accompanying the reactions reflected conformational adjustments of the polymer which influence the nearest environment and thus the ligand fields of the Ni(II) centers, as observed earlier for simpler metal DBM complexes.^{34,87,88}

Inspection under the microscope of the solid $[\text{Ni}(\text{bipy})(\text{DBM})_2]$ suspended in various solvents revealed that in some cases at least a two-step inclusion process occurs. One such example is illustrated in Figure 7. In the first five minutes in bromobenzene (50 °C) the host phase

(polymorph I) transforms into a metastable single-phase product in the form of isometric crystals 5–10 μm in size. In the next 10 min the crystals convert into the final product in the form of needles. No more transformation or crystal growth is observed afterward. The reaction with *p*-xylene also goes through a metastable product (type V in Table 3) but it takes up to 1 day to go to a final product (type IV in Table 3).

Crystal Structure of $[\text{Zn}(\text{bipy})(\text{DBM})_2] \cdot 2(\text{Chlorobenzene})$. No crystals containing $[\text{Ni}(\text{bipy})(\text{DBM})_2]$ and suitable for single-crystal XRD study were obtained, but it was possible to isolate and study a single crystal of the $[\text{Zn}(\text{bipy})(\text{DBM})_2] \cdot 2(\text{chlorobenzene})$ inclusion compound which is isostructural to its nickel counterpart⁸⁹ (type IV in Table 3). The compound exhibits van der Waals packing of 1D host polymeric chains and guest molecules. Crystallographic parameters of the structure are listed in Table 1.

A fragment of the host polymeric chain is shown in Figure 8a. The Zn center is bonded to six donor atoms with average angular deviation from a regular octahedral environment of 1.5°. Two DBM ligands chelate the Zn center in the equatorial plane with Zn–O distances ranging from 2.055 to 2.063 Å. The bipy ligands bridge two zinc centers with Zn–N distances of 2.175 and 2.202 Å. It is interesting that the chelate semi-rings (O1, C1, C2, C3, O3 and O4, C4, C5, C6, O6) deviate from the equatorial plane of the complex forming a dihedral angle of as much as 30.3° to each other. These distortions in the nearest coordination environment of the metal center seem to be defined by the guest and are responsible for the color variations among inclusion compounds of the nickel polymer.

The host polymeric chain may be modeled as a “wheel-and-axle” sequence of flat metal DBM units connected by rigid bipy spacers. The distance between adjacent metal DBM units ($\text{Zn} \cdots \text{Zn}$) is 11.45 Å. The “pockets” located near bipy between “wheels” are 6 Å deep and 8–10 Å long.

The chains run parallel to each other (Figure 8b); two chains pass through the unit cell parallel to the (ac) plane at $y = 0.25$ and 0.75 . The chains lying on the same y -level interdigitate, partially filling each others pockets with phenyl fragments. The rest of the pocket space is combined into cavities available for guest chlorobenzene. Guest molecule A occupies a cavity between chains on the same y -level. Guest molecule B, which is disordered, occupies a larger cavity between the chains at $y = 0.25$ and $y = 0.75$. The cavities are connected to each other forming a channel along the *a* crystallographic axis.

Presumably, all nickel compounds studied in this work have the same host polymeric chain motif as found in $[\text{Zn}(\text{bipy})(\text{DBM})_2] \cdot 2(\text{chlorobenzene})$. The variety of crystal structures observed arises from displacement of the parallel polymeric chains with respect to each other creating cavities of a suitable geometry for every particular guest. It should be noted also that formation or expansion of cavity space in coordination polymers of higher dimensionality was recently observed, as a result of an appropriate displacement of 2D⁹⁰ and 3D^{28,91} host networks.

(87) Soldatov, D. V.; Ripmeester, J. A. *Supramol. Chem.* **2001**, *12*, 357–368.

(88) Soldatov, D. V.; Enright, G. D.; Ripmeester, J. A. *Chem. Mater.* **2002**, *14*, 348–356.

(89) Guest-free form of $[\text{Zn}(\text{bipy})(\text{DBM})_2]$ was structurally different from both guest-free polymorphs of the nickel compound, and it did not show the ability to absorb methane or xenon.

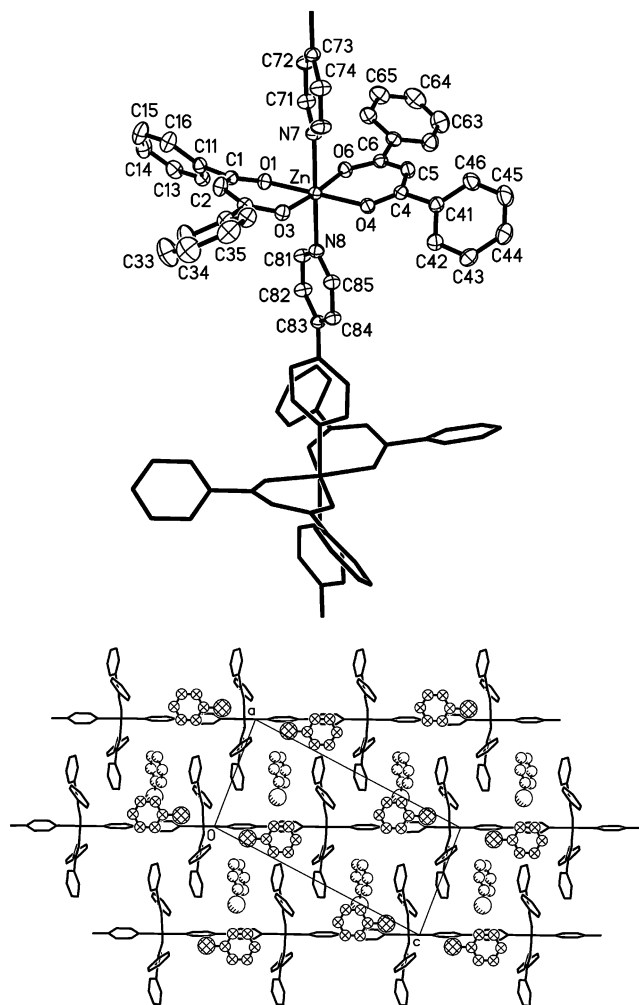


Figure 8. Crystal structure of the $[\text{Zn}(\text{bipy})(\text{DBM})_2] \cdot 2\text{-(chlorobenzene)}$ inclusion compound. (a) Two adjacent monomer units of the host chain; the thermal ellipsoids (probability of 50%) and numbering scheme are shown for the host asymmetric unit. (b) Projection of the structure along *b* (half unit cell content). Guest molecules are outlined as ball-and-stick models, shaded circles for molecule A and crosshatched circles for molecule B.

Deuterium NMR of $[\text{Ni}(\text{bipy})(\text{DBM})_2] \cdot x(\text{C}_6\text{D}_6)$. ^2H NMR spectra are shown in Figure 9. Although sample A (dried superficially) appeared relatively dry, its ^2H NMR spectrum shows a sharp component and a broad component in the 296 K spectrum (Figure 9b) with intensities roughly in the ratio 4:3. On cooling, it becomes apparent that the sharp line is from liquid benzene. In the 280 to 273 K region the narrow component is drastically reduced and replaced by a doublet line shape superimposed on and slightly broader than the other broad component (see the 273 K spectrum in Figure 9c). Such a rapid change in line shape is indicative of a phase change and the temperature region corresponds quite well with the known melting point of pure C_6D_6 of 278 K.

A bulk sample (0.4 g) prepared following the same procedure as that used for sample A showed a mass loss in air corresponding to 4.7 mol of benzene. Taking the

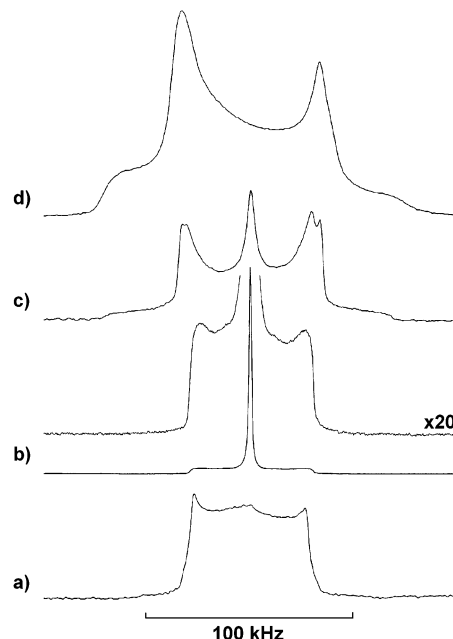


Figure 9. ^2H NMR spectra of $[\text{Ni}(\text{bipy})(\text{DBM})_2] \cdot x(\text{C}_6\text{D}_6)$: (a) "dry" sample B at 296 K; (b–d) "wet" sample A at 296 K (b), 273 K (c), and 77 K (d).

ratio 4:3 of liquid/included benzene, the guest-to-host molar ratio in the compound can be roughly estimated to be 2.0. Note, however, that the intensity from included benzene may be underestimated because of dynamics.

The dried sample B shows only the broad component at 296 K (Figure 9a). As this is not a distinct quadrupolar line shape this benzene is probably undergoing dynamic averaging at some intermediate rate. What is most revealing about this line shape (and the same component in sample A) is that the distinct features are not symmetrical about the center (given by the liquid line). This is due to weak dipolar interactions with the paramagnetic Ni(II), and demonstrates relatively close proximity between benzene and these centers.^{92,93} Thus, it is quite clear that this is guest benzene inside the pores of the material presumably formed by "pockets" between flat metal DBM units. In contrast, the doublet from the bulk benzene that appears after the liquid freezes is symmetrical about zero, indicating the lack of proximity between these benzenes and the paramagnetic centers.

The width of the bulk benzene doublet (effective quadrupole coupling constant $C_Q = 91.8$ kHz at 273 K) is characteristic of rapid in-plane reorientation of the benzene⁹⁴ with some further narrowing caused by out-of-plane librational motions. The 77 K spectra of samples A (Figure 9d) and B obtained with an experimental recycle time of 0.35 s were essentially identical, and show only the benzene inside the complex, still under-

(90) Kitaura, R.; Seki, K.; Akiyama, G.; Kitagawa, S. *Angew. Chem., Int. Ed.* **2003**, *42*, 428–431.

(91) Chen, B.; Fronchek, F. R.; Maverick, A. W. *Chem. Commun.* **2003**, 2166–2167.

(92) Ratcliffe, C. I.; Soldatov, D. V.; Ripmeester, J. A. *Microporous. Mesoporous Mater.* accepted for publication.

(93) It is not possible to extract quantitative information about the benzene–Ni(II) distances from the NMR spectra, but it might be reasonable to suggest distances similar to those seen between chlorobenzene and Zn(II) in the crystal structure which was determined in this work. The Zn–H(chlorobenzene) distances range within 4.2–7.9 Å for guest A and 5.1–8.2 Å for disordered guest B.

(94) Ok, J. H.; Vold, R. R.; Vold, R. L.; Etter, M. C. *J. Phys. Chem.* **1989**, *93*, 7618–7624.

going rapid in-plane reorientation. The short recycle time discriminates against bulk benzene, which is static at 77 K and thus has a line which is twice as broad and also has a very long spin–lattice relaxation time.⁹⁴ The paramagnetic distortions are more evident than at 296 K, presumably because of temperature-dependent paramagnetism, again indicating the presence of nearby Ni(II) centers. Evidence of a second motion for the guest benzene in addition to in-plane rotation is apparent at 150 K and above, where the line shape narrows further. Unfortunately, it is not possible to determine the exact details of this motion, as the fast limit does not appear to have been reached at 296 K.

Conclusions

This work qualifies the title polymeric complex, [Ni(bipy)(DBM)₂], as a new sorbent material with a dynamic (adaptable to the guest and external conditions) metal–organic framework. This material presents special problems for characterization, as single crystals of suitable size could not be grown, and paramagnetism interferes with the usual NMR spectroscopic applications. However, the general approach employed, that of structural analogy, along with the examination of the adsorbed guests by NMR spectroscopic methods defines the material adequately.

The [Ni(bipy)(DBM)₂] complex behaves as a microporous sorbent with a versatile ability to absorb gases and organic solvents. This conclusion follows from all of the various experiments reported in this work. The amount of guest included is variable from zero to more than two moles per host monomer unit. Direct evidence that the absorbed species are included in the crystal lattice of the material comes from ¹²⁹Xe and ²H NMR experiments.

The sorption capacity of the [Ni(bipy)(DBM)₂] material with respect to gases was determined to be 67 mL/g (STP) for xenon (298 K, 60 atm) and at least 27 mL/g for methane (298–423 K, 110–127 atm). These quantities are significant taking into account the relatively high temperatures of the sorption process. For comparison, other sorbents show the following capacity at room or higher temperatures: (1) zeolite NaX, 88 mL/g (methane, 323 K, 50 atm);⁹⁵ (2) zeolite 13X, 40 mL/g (methane, 298 K, 36 atm);²² (3) [M₂(bipy)₃(NO₃)₄], 52 mL/g (methane, 298 K, 30 atm),²² 9 mL/g (argon, 273 K, 1 atm);²³ (4) [Co₂(azpy)₃(NCS)₂] (azpy = 4,4'-azopyridine), 15 mL/g (methane, 298 K, 36 atm);⁹⁵ (5) [Cd₂(azpy)₃(NO₃)₄], 40 mL/g (methane, 298 K, 36 atm);⁹⁶ (6) {Cu(*p*-OOC–C₆H₄–COO)(bipy)_{0.5}}_n, 47 mL/g (methane, 353 K, 30 atm);²⁸ (7) syndiotactic polystyrene, 21–29 mL/g (carbon dioxide, 298 K, 25 atm; assuming density of the material is ~1 g/cm³).⁴⁴ Zeolites (1) and (2) are

materials with essentially robust, unchangeable frameworks. Materials (3) and (4) are metal–organic and also possess robust frameworks; that is, no deformation of the crystal framework is observed during sorption. Material (5) has a flexible metal–organic framework but still retains porosity in the absence of sorbate. Material (6) has a very flexible metal–organic framework made up of two interpenetrated 3D frameworks; this material acquires porosity only when subjected to a significant guest pressure. Material (7) is a highly flexible organic polymer with a structure resembling that of the material of this study. Overall sorption in material (7) is, in fact, a sum of sorption and dissolution, which are approximated by Langmuir's and Henry's laws, respectively. As may be seen from the above comparison, the sorption capacity of most recently designed flexible frameworks is comparable to that of the well-known robust structures. In an overall comparison of these materials, the novel properties of the flexible sorbents, such as controlled assembly–disassembly, adaptability, and the possibility to change sorption properties by an external control, bring advantages that should not be overlooked.

The crystal structure of the complex is very flexible, producing a variety of structurally distinct inclusion materials. This “flexibility” of the crystal lattice seems to be an intrinsic property of the host complex. The basic structural features of the complex are very similar to those of its isostructural zinc analogue, as illustrated by the [Zn(bipy)(DBM)₂]*2(chlorobenzene) inclusion compound, also studied here. The sequence of flat metal DBM units bridged with bipy spacers resembles the “wheel-and-axle” supramolecular design applied earlier to organic host molecules. There are evident advantages in applying this design to metal complexes, such as easier synthesis and easier modification.

Presumably, the 1D polymeric structure of the complex is retained in all of its inclusion compounds, but the packing of the polymeric chains in the other two dimensions occurs in different ways, resulting in the observed variability of inclusion structures. The combination of relatively high thermal stability of the title material and its easy transformation into various supramolecular architectures suggests a new design strategy for versatile sorbents with novel properties.

Acknowledgment. The contributions of P. Tinne-mans and P. R. Diamente, who assisted in preliminary experiments, are gratefully acknowledged. Useful comments from G. D. Enright are greatly appreciated.

Supporting Information Available: Final fractional atomic coordinates and other structural data for [Zn(bipy)(DBM)₂]*2(Chlorobenzene) (CIF file). This material is available free of charge via the Internet at <http://pubs.acs.org>.

(95) Zhang, S.-Y.; Talu, O.; Hayhurst, D. T. *J. Phys. Chem.* **1991**, 95, 1722–1726.

(96) Kondo, M.; Shimamura, M.; Noro, S.; Minakoshi, S.; Asami, A.; Seki, K.; Kitagawa, S. *Chem. Mater.* **2000**, 12, 1288–1299.